Enzyme and Microbial Technology 100 (2017) 60–70

Contents lists available at ScienceDirect

Enzyme and Microbial Technology

journal homepage: www.elsevier.com/locate/emt

One-step combined focused epPCR and saturation mutagenesis for thermostability evolution of a new cold-active xylanase

Juan Pablo Acevedo[c], Manfred T. Reetz[d,e], Juan A. Asenjo[f], Loreto P. Parra[a,b,*]

[a] Institute for Biological and Medical Engineering, Schools of Engineering, Medicine and Biological Sciences, Pontificia Universidad Católica de Chile, Avenida Vicuña Mackenna, 4860 Santiago, Chile
[b] Department of Chemical and Bioprocesses Engineering, School of Engineering, Pontificia Universidad Católica de Chile, Avenida Vicuña Mackenna, 4860 Santiago, Chile
[c] Facultad de Medicina y Facultad de Ingeniería y Ciencias Aplicadas, Universidad de los Andes, San Carlos de Apoquindo, 2200 Santiago, Chile
[d] Max-Planck-Institut für Kohlenforschung, 45070 Mülheim, Germany
[e] Chemistry Department, Philipps-University, 35032 Marburg, Germany
[f] Centre for Biotechnology and Bioengineering, CeBiB, Department of Chemical Engineering and Biotechnology, University of Chile, Beauchef, 851 Santiago, Chile

ARTICLE INFO

Article history:
Received 26 August 2016
Received in revised form 25 January 2017
Accepted 9 February 2017
Available online 13 February 2017

Keywords:
Xylanase
Cold-active enzymes
Thermostability
Directed evolution
epPCR

ABSTRACT

Enzymes active at low temperature are of great interest for industrial bioprocesses due to their high efficiency at a low energy cost. One of the particularities of naturally evolved cold-active enzymes is their increased enzymatic activity at low temperature, however the low thermostability presented in this type of enzymes is still a major drawback for their application in biocatalysis. Directed evolution of cold-adapted enzymes to a more thermostable version, appears as an attractive strategy to fulfill the stability and activity requirements for the industry. This paper describes the recombinant expression and characterization of a new and highly active cold-adapted xylanase from the GH-family 10 (Xyl-L), and the use of a novel one step combined directed evolution technique that comprises saturation mutagenesis and focused epPCR as a feasible semi-rational strategy to improve the thermostability. The Xyl-L enzyme was cloned from a marine-Antarctic bacterium, *Psychrobacter* sp. strain 2–17, recombinantly expressed in *E. coli* strain BL21(DE3) and characterized enzymatically. Molecular dynamic simulations using a homology model of the catalytic domain of Xyl-L were performed to detect flexible regions and residues, which are considered to be the possible structural elements that define the thermolability of this enzyme. Mutagenic libraries were designed in order to stabilize the protein introducing mutations in some of the flexible regions and residues identified. Twelve positive mutant clones were found to improve the T_{50}^{15} value of the enzyme, in some cases without affecting the activity at 25 °C. The best mutant showed a 4.3 °C increase in its T_{50}^{15}. The efficiency of the directed evolution approach can also be expected to work in the protein engineering of stereoselectivity.

© 2017 Elsevier Inc. All rights reserved.

1. Introduction

Microorganisms living in cold environments have developed structural adaptations on their proteins to compensate and overcome the effects of low temperatures. These special features make psychrophilic organisms very interesting for the identification and isolation of novel cold-active enzymes [1–4]. The use of enzymes with higher activity at low temperatures allows energy savings in industrial biocatalysis by lowering the required temperature of a reaction without sacrificing enzyme activity. Cold-adapted enzymes can also prevent undesirable chemical reactions occurring at higher temperatures and exhibit a rapid heat-inactivation derived from their structural thermolability, which is of special interest in the food industry [5–9]. In spite of these important advantages, the stability of a cold-active enzyme in a biocatalytical process is still a drawback. A stable enzyme can tolerate the presence of solvents or other reagents, high temperatures and extreme pH, common conditions affecting the folding integrity of proteins or enzymes in industrial processes [10]. Therefore, the use of protein engineering to improve the stability of enzymes has a high significance for industry and basic research [11,12]. Among protein engineering techniques, directed evolution utilizes random

Abbreviation: GH, glycosyl hydrolases.

* Corresponding author at: Institute for Biological and Medical Engineering, Schools of Engineering, Medicine and Biological Sciences, Pontificia Universidad Católica de Chile, Avenida Vicuña Mackenna 4860 Santiago, Chile.
E-mail addresses: lparrat@uc.cl, lparraa@ing.puc.cl (L.P. Parra).

http://dx.doi.org/10.1016/j.enzmictec.2017.02.005
0141-0229/© 2017 Elsevier Inc. All rights reserved.

or semi-rationally guided mutagenesis, meaning that no or little protein structural knowledge is needed. This approach involves iterative cycles of gene mutagenesis and protein expression, followed by screening assays in order to find enzyme variants with optimized properties; subsequently the process can be repeated and mutations can often be combined to further improve the properties [13–16]. Directed evolution is one of the most effective approaches to engineer enzyme stability [17,18]. The typical strategies applied when no detailed structural information of the enzyme is available are error-prone PCR [19] and DNA shuffling [20]. On the other hand, the most common knowledge-driven approach is saturation mutagenesis or cassette mutagenesis, where a given site of a protein, comprising one or more amino acids, is randomized by the introduction of all 20 canonical amino acids [21,22].

After the creation of directed evolution techniques based on purely random [23,24] (e.g. epPCR, DNA shuffling) or semi-rational methodologies [25–27] (e.g. saturation mutagenesis, CAST, Iterative Saturation Mutagenesis/B-factor), scientists have evolved in the laboratory several industrially relevant enzymes to obtain variants with higher activity at lower temperature. These methodologies have been mostly applied to meso- and thermophilic enzymes to be able to catalyze reactions at low temperatures, and to a lesser extent to cold-active enzymes for increasing their thermal stability without affecting high activity at low temperature. These are usually more challenging to evolve due to the reduced tolerance to accept mutations without affecting stability or activity [28]. Successful examples of both alternatives were recently reviewed [9], revealing that directed evolution techniques employing extended epPCR cycles, DNA shuffling [29] and family shuffling [30] have been used most often, although strategies targeting rigid and flexible regions within proteins appear to be more rational. In this regard, the identification of amino acids with high flexibility can be performed using the B-FITTER computer aid (www.kofo.mpg.de/en/research/biocatalysis), which extracts the B-Factor values from pdb-files [17]. However, punctual mutations targeting amino acids showing high flexibility are sometimes not enough to increase local rigidity, and should be accompanied by co-mutations targeting surrounding residues in order to induce synergistic anchoring effects for structural stabilization.

Xylanases are glycosyl hydrolases (GH) normally reported as members of the particular GH-families 10 and 11 (GH10 and GH11 xylanases respectively) [31]. Xylanases hydrolyze the β-1,4 backbone of the major constituent of hemicellulose, xylan, which makes them an attractive group of biocatalysts for industry [32]. The major xylanase-mediated industrial processes are found in the pulp, paper and cellulosic ethanol production [33]. Among cold-active xylanases that have been identified, only a small number have been purified and characterized, showing common characteristics such as high catalytic activities at low temperatures and poor thermal stability [31].

Using directed evolution strategies, thermostability of xylanases has been improved [34]. However, most of the improvements were achieved for mesophilic enzymes belonging to GH11 and using epPCR or saturation mutagenesis as protein engineering strategies [35]. Nevertheless, GH10 xylanases have larger substrate scopes than its GH11 congeners, which, apart from D-xylose derived substrates, include low molecular mass celluloses and aryl cellobiosides [31]. GH11 xylanases also show less versatility in catalysis than GH10 xylanases [36,37]. Therefore, improvement of GH10 xylanases, showing higher thermal stability and catalytic efficiency on various substrates, is of great importance in different industrial sectors.

This work describes the use of a one-step combined saturation mutagenesis and region-focused epPCR as a feasible semi-rational directed evolution strategy to improve the thermostability of a new cold-active xylanase (Xyl-L), overcoming the intrinsic difficulties of evolving thermostability of enzymes with low thermal stability. Additionally in this work, a novel cold-active xylanase isolated from the Antarctic seawater bacterium *Psychrobacter* sp. strain 2–17 [38], previously cloned and recombinantly expressed [39], was characterized. We performed focused epPCR [40] with simultaneous saturation mutagenesis in regions showing high degrees of flexibility. As will be seen, this enables the improvement of thermostability between 1 and 4 °C in the T_{50}^{15} value of Xyl-L, while maintaining catalytic activity at low temperatures. The simultaneous combination of focused epPCR and saturation mutagenesis at flexible residues proved to be more efficient in finding better variants than the solely saturation mutagenesis at the most flexible residues in a cold-active xylanase.

2. Materials and methods

2.1. Material, strains, vectors and culture conditions

Elongase and T4 DNA ligase were supplied by Invitrogen. Restriction enzymes were obtained from New England Biolabs. *Taq* DNA polymerase was purchased from Promega. KOD hot start Polymerase, 10X KOD Buffer, dNTPs and $MgSO_4$ were supplied by Novagen. DNA sequencing was done by Macrogen (Korea) and Eurofins. Primers were synthesized by Eurofins and Invitrogen. Birchwood xylan was obtained from Sigma. TB medium, LB medium, marine medium 2216 and granulated agar were acquired from Difco. Tris, SDS and glycerol were purchased from Winkler. *Psychrobacter* sp. strain 2–17 was isolated from Antarctic-seawater as previously described [38]. *Escherichia coli* strain DH5α was used as the recipient strain for plasmids with genes encoding or partially encoding recombinant xylanase protein and was obtained from Invitrogen. *E. coli* strain BL21(DE3) and pET-22b(+), used as bacterial host and expression vector respectively, were obtained from Invitrogen. Cells for genomic DNA manipulation were harvested 4 days after cultivation in marine medium 2216 with shaking (200 rpm) at 4 °C.

2.2. Gene cloning and recombinant expression

A sense primer LF1 (5′-TGTTTTTTCATGGCGGCGG-3′) and an antisense primer LF2 (5′-GGCGATAGTGCCGGCGG-3′) were able to amplify a central region of the xylanase encoding gene from *Psychrobacter* sp. strain 2–17 using *Taq* DNA polymerase and the conditions reported by Parra et al. (2008) [38]. The amplification products were cloned in a pGEM-T easy system and sequenced. The complete xylanase encoding gene was obtained using a genome walking method previously described [39]. A forward primer to amplify the 3′ end (5′-GATGCAAAGTTTTCAAGGTGATAAAGCCG-3′) and a reverse primer to amplify the 5′ end (5′-CCATAAACGCTTCGTTAACTACATCCCAG-3′) were used as first specific primers. For the second round of PCR, a forward primer to amplify the 3′ end (5′-CTGGGATGTAGTTAACGAAGCGTTTATGG-3′) and a reverse primer to amplify the 5′ end (5′-CGGCTTTATCACCTTGAAAACTTTGCATC-3′) were used as second specific primers. Primers XylFo (5′-CTTTCCATGGCGTGCGGGGGGAATAATAAAG-3′ and XylRe (5′-TAGGCTCGAGTTCGACCAAGGTTACCG-3′), carrying a *Nco*I and *Xho*I restriction site respectively, were used to amplify a 1222 bp fragment encoding the xylanase gene directly from the genomic DNA of *Psychrobacter* sp. strain 2–17, using Elongase. The thermal cycling conditions were; 5 min at 95 °C; 25 cycles consisting of 35 s at 94 °C, 45 s at 62 °C and 2.5 min at 68 °C; and 1 final additional step at 72 °C for 10 min. After digestion with *Nco*I and *Xho*I, the PCR product was ligated with the pET-22b(+) vector forming the recombinant plasmid Xyl-L-pET. *E. coli* BL21 (DE3) electrocom-

petent cells were transformed with the recombinant plasmid. The clones producing the highest levels of xylanase activity were chosen based on the Congo red-polysaccharide interactions [41]. One selected positive colony was grown in 250 ml of TB medium containing 100 μg/ml of carbenicillin (CB) at 37 °C with shaking. When an optical density of 0.5 at 600 nm was reached, isopropyl-β-D-thiogalactopyranoside (IPTG) with a final concentration of 0.3 mM was added, and the growth temperature was lowered to 18 °C. After 40 h of cultivation, cells were removed by centrifugation at 10000 × g for 10 min at 4 °C for enzyme purification from the supernatant. Ammonium sulfate was added to the supernatant to a final concentration of 80% (w/v). The solution was incubated with shaking at 4 °C for 12 h. The precipitate was collected by centrifugation and dissolved in binding buffer (50 mM NaH_2PO_4, 300 mM NaCl, 10 mM Imidazole) followed by dialysis against the same buffer at 4 °C for 12 h. For purification from the periplasm, the induction with IPTG was done for 24 h at 18 °C and cells were collected by centrifugation at 5000 × g for 5 min at 4 °C. Periplasm collection was performed following instructions provided in the handbook for purification of 6xHis-tagged proteins from "The QIAexpressionist" manual (Qiagen, USA). The protein solutions were applied to a Ni-NTA column equilibrated with binding buffer. The elution was performed at a flow rate of 0.5 ml/min with elution buffer (binding buffer 250 mM imidazole). Aliquots eluted from the column were used for biochemical characterization.

2.3. Characterization of Xyl-L

SDS-PAGE was performed using 12% acrylamide gels. Protein concentration was determined according to Bradford [42]. Activity of the purified enzyme was determined measuring the amount of reducing sugars liberated from 1.5% soluble birchwood xylan at pH 8 and different temperatures. Briefly, 50 μl of assay buffer (3% birchwood xylan in buffer Tris/HCl 50 mM, $CaCl_2$ 2 mM, pH 8) were mixed with 50 μl of supernatant sample. After 20 min, the reaction was stopped by adding 100 μl of DNS reagent [43] into 100 μl of reaction. The samples were heated for 5 min at 100 °C and then cooled to 4 °C for 10 min and OD_{550} was measured. Enzyme parameters k_{cat} and K_m were determinated by regression analysis of the Michaelis-Menten equation. Birchwood xylan was used as the substrate at concentrations between 0 and 32 mg/ml. All the measurements were made in triplicate. The effect of the pH on the reaction rate was determined by measuring xylanase activity at different pH values at room temperature using a 100 mM Britton and Robinson buffer [44] in the range of 4–10. Thermostability was determined obtaining $T_{50}{}^{15}$ (50% activity after 15 min at the defined temperature) values for the expressed mutant enzymes by measuring the residual activity after the heat shock at temperatures ranging from 30 to 45 °C. Measurements for the activation energy calculation were carried out starting the reaction by the addition of the enzyme at different temperatures between 5 and 30 °C. The k_{cat} and K_m values, obtained from the determination of the initial reaction rates at different concentrations of substrate, using a constant enzyme concentration, were calculated for each temperature. Effects of metal ions on the Xyl-L activity were examined by adding 1 and 10 mM of $ZnSO_4$, $CoCl_2$, $NiCl_2$, $CuCl_2$, $MnCl_2$ and $CaCl_2$. Also EDTA (1 and 10 mM), SDS (1 and 10%) and TritonX-100 (1 and 10%) effects were studied. The substrate was added after incubating the enzyme with each metal ion, chelating agent or surfactant for 30 min at 25 °C, and the reaction was performed for 20 min.

2.4. Three-dimensional modeling of Xyl-L and molecular dynamics (MD) simulations

A homology model of the catalytic domain of Xyl-L was built using the MODELLER software [45]. The model was developed using three previously described xylanase structures from family 10 of glycosyl hydrolases. The structures included were: xylanase A from *Streptomyces halstedii* JM8 (1NQ6) [46], with 34% identity; xylanase XYN10A from *Cellvibrio japonicus* (1W32) [47] with 41% identity; xylanase 10C from *Cellvibrio japonicus* (1US2) [48] with 41%. The molecular structures were manipulated with the program Swiss-Pdb Viewer [49]. The nucleotide sequence of the gene encoding Xyl-L from *Psychrobacter* sp. 2–17 has been patented [50] and the sequence has been deposited with the GenBank accession number HH759472 (*GenBank: HH759472*). The in-silico structure manipulations and molecular dynamics simulations were performed using the Schrödinger software as described by Wu and coworkers [51]. Briefly, A Polak-Ribier conjugate gradient with a convergence threshold on the gradient of 0.05 kJ/Å/mol was used for the minimization of the structures. The selected force field for minimization was OPLS_2005, and the surface area-based version of the generalized born (GB/SA) model was used for treatment of solvent (water), and its dielectric constant was assigned a value of 1. In order to generate the solvated systems for dynamic simulations, a cubic periodic unit cell containing 70524 water molecules, 120 Na+ ions, and 120 Cl- ions was used. This solvent cube was defined by adding a minimum layer of 20 Å buffer molecules from the protein surface, having 0.15 M NaCl. All simulations used the SPC water model, and the OPLS-AA force field for protein. Long-range electrostatic interactions using Particle Mesh Ewald (PME) and van der Waals interactions were computed with a real space contribution truncated at 9 Å. Bond lengths to hydrogens were constrained using the SHAKE algorithm. A RESPA integrator with time steps set to 2 fs for bonded and short-range nonbonded interactions was used, and to 6 fs for long-range electrostatic interactions. Before every dynamic simulation, the solvated systems were relaxed into a local energy minimum using 50 steps of a hybrid method of steepest descent minimization and a limited-memory Broyden-Fletcher-Goldfarb-Shanno (LBFGS) minimization. Additionally, the model systems were relaxed before simulation through a series of minimization and short dynamic simulations (NPT ensemble using a Berendsen thermostat and barostat) equilibrating the system at 300 K and 1 bar. Finally, production simulation was performed for the solvated system during 2 ηs, coupling the system using NPT simulation, maintaining 1 Atm at 300 K with a Martyna-Tobias-Klein barostat (relaxation time of 2 ρs) and a Nose-Hoover thermostat (relaxation time of 0.5 ρs). MD simulation was performed with the Desmond program using an algorithm for high-speed parallel execution, recording conformations every 1.2 ρs [52]. The average RMSD was calculated for each residue using the simulation frames from the last 1 ns of the MD simulation using a molecular graphics program VMD [53].

2.5. Mutagenesis libraries design

The basic concept of the new directed evolution technique involves simultaneous one-step epPCR focused on a specified region of an enzyme and saturation mutagenesis at rationally chosen residues (see Scheme S1 in the Supplementary Material). As template, a Xyl-L variant with a punctual mutation; P35L (Xyl-L-310B), was used. This mutant shows a 2.3 fold increase in k_{cat} compared to the WT xylanase and no differences in K_m, and it was obtained after one round of epPCR experiments (data not shown).

Two different sets of mutagenic libraries were designed and fabricated: Saturation Mutagenesis (SM) libraries (Libraries A and B), and epPCR + saturation mutagenesis libraries (Libraries C, D and E).

i) SM libraries were created with a codon degeneracy obtained by a mixture of NDT, VHG, and TGG codons as described before [54]. Since in both libraries (A and B) the two randomized amino acids were located within less than 1 amino acid distance in the

coding nucleotide sequence, a mixture of 18 mutagenic primers (9 forward and 9 reverse; supporting information) was used in a QuikChange™ Site-Directed Mutagenesis reaction [55]. The amplification reaction contained in a total volume of 50 μl; 10 x KOD Buffer, dNTPs 2 mM each, $MgCl_2$ (25 mM), mutagenic primers (250 ng), template plasmid (50 ng), and KOD Hot start polymerase (0.5 U). PCR conditions were; 1 cycle at 94 °C for 2 min; 25 cycles of 94 °C for 50 s, 65 °C for 50 s and 72 °C for 8 min and a final additional extension step at 72 °C for 10 min

ii) Focused epPCR + SM libraries were obtained after performing the randomization of 2 amino acids using separated mutagenic primers, therefore an amplified megaprimer is generated and isolated, having the randomized nucleotides at the specific location. Likewise, focused epPCR is performed to obtain and isolate a second megaprimer harboring randomly distributed mutations at a calculated frequency of 3 mutations per 120 pb. Both megaprimers are combined in a third PCR reaction using the described megaprimer methodology [56] (see Fig. 1). Focused epPCR was performed using the GeneMorph II EZCLone Domain Mutagenesis Kit according to the manufacturer's manual (Agilent Technologies). Two flexible regions in the catalytic domain were chosen for the epPCR; from position E135 to L167 (primers EPXIL135-167F2 and EPXIL135-167R2, supporting information) and from position R244 to E276 (primers EPXIL244-276F2 and EPXIL244-276R2, supporting information). After primers alignment during the focused epPCR, one of the sequence sections was subjected to random mutagenesis including the nucleotides coding the amino acids from position 243–277. In the second focused epPCR, the randomized nucleotides included those coding from the amino acid at position 134 to position 168. To standardize the conditions for focused epPCR, different template concentrations were evaluated. The final amplification reaction contained in a total volume of 50 μl: 10 × Mutazyme II reaction buffer, dNTP mix 200 μM each final, primers (forward and reverse 125 ng each), template plasmid (0.1 ng), Mutazyme II DNA polymerase (2.5 U). The thermal cycling conditions were; 2 min at 95 °C; 30 cycles consisting in; 30 s at 95 °C, 30 s at 60 °C and 1 min at 72 °C; and a final additional extension step at 72 °C for 10 min. SM libraries were also created with a codon degeneracy generated by a mixture of NDT, VHG, and TGG codons [54]. A mixture of 6 mutagenic primers (3 forward and 3 reverse; supporting information) was used in a single two-stage whole-plasmid PCR [56]. The PCR conditions for the saturation mutagenesis were; 1 cycle at 94 °C for 2 min; 8 cycles of 94 °C for 30 s, 65 °C for 1 min and 72 °C for 1 min; 25 cycles of 94 °C for 30 s and 72 °C for 45 s; 1 final additional cycle at 72 °C for 10 min. Both PCR products were purified and used as megaprimers in a QuikChange reaction for the amplification of the xylanase gene containing plasmid. The PCR conditions were; 1 cycle at 94 °C for 2 min; 25 cycles of 50 s at 94 °C, 50 s at 65 °C and 15 min at 72 °C, and a final additional extension step at 72 °C for 10 min

The PCR products were digested with *Dpn*I to hydrolyze the template plasmid by adding 2 μl *Dpn*I directly to the PCR product and incubating the reaction at 37 °C for 2 h. The sample was used for transformation by electroporation of *E. coli* BL21(DE3) electrocompetent cells. The integrity and quality of the coding region was verified by DNA sequencing as previously described [54].

2.6. Libraries expression and screening

For each library 1472 individual colonies were randomly picked using a colony picker QPIX (Genetix, Boston, MA) and used to inoculate sixteen 2.2 ml 96-deep-well plates containing TB media (800 μl) supplemented CB (100 μg/ml) per well. Four wells in the last column of the 16 plates were inoculated with the parental strain, resulting in 1536 colonies per library. Library expression was performed as described previously [27]. Induction was performed by adding 100 μl of an IPTG solution in TB medium 6.3 mM (final concentration in each well; 0.7 mM IPTG). The expression was performed at 18 °C for 40 h. The cells were harvested by centrifugation (4000 rpm, 15 min) and the supernatant was used for the screening. Screening was performed by measuring the activity at room temperature (20–25 °C) and the residual activity. For this purpose a 96-head pipetting robot (Tecan) was used to dilute the supernatants 1:1 in buffer (Tris/HCl, 2 mM $CaCl_2$ pH 8) in a total volume of 50 μl in 96-microtiter plates. The heat shock was performed at 42 °C for 7 min using a 96 well plate heater and stopped by cooling the plates at 4 °C for 10 min. The samples were kept at room temperature for 15 min before adding the substrate. The residual enzyme activity was determined by adding 50 μl of 3% soluble birchwood xylan in Tris/HCl, 2 mM $CaCl_2$ buffer, pH 8, at 25 °C, before and after the heat shock. Positive clones were detected calculating the percentage of retained activity. Reproduction of the cultures was performed for each potential hit as described by Reetz and Carballeira [27].

The best mutants and the parental enzyme Xyl-L–310 B were purified and the thermostability was determined by T_{50}^{15} values as described above.

3. Results

3.1. Cloning and sequencing of the xylanase-encoding-gene

A partial xylanase gene (240 bp) from a glycosyl hydrolase family 10 (GH10) was amplified from the genomic DNA of *Psychrobacter sp*. strain 2–17 using primers LF1 and LR1. The xylanase encoding gene was completed by genome walking [39] obtaining an open reading frame of 2220 bp coding for a 740 amino acid protein (Xyl-L). The primary structure of the enzyme was analyzed, identifying a 20 residue signal peptide and two carbohydrate binding domains flanking the catalytic domain. The Xyl-L amino acid sequence was compared with those of other xylanases in the NCBI database finding 94 and 93% of identity with two family GH10 xylanases from different *Pseudoalteromonas* sp. (unpublished). Based on the conserved residues in the multiple sequence alignment of other GH10 xylanases, Xyl-L probably uses the catalytic residues E368 and E486. Xyl-L has an apparently high molecular mass of approximately 90 kDa and a predicted low pI of 4.24. These characteristics are typically found in *endo*-β-1,4-xylanases of family 10 which have a high molecular mass, a low pI and display an (α/β)8 barrel fold [31].

3.2. Expression and characterization of Xyl-L

The *xyl-L* gene was expressed using the *E. coli* BL21*(DE3)/pET-22b(+)* expression system. The recombinant Xyl-L was overproduced in the supernatant and periplasm in a catalytically active form with a higher purity detected in the periplasm; therefore the characterization of the recombinant enzyme was performed using the purified periplasmic fraction and birchwood xylan as the substrate.

The temperature activity profile of Xyl-L was examined in the range of 4–50 °C at pH 8. As expected for a cold-active enzyme, Xyl-L shows above 50% of its maximum activity at temperatures between 15 and 40 °C. 35 °C is the temperature where its maximum activity is observed (Fig. 2A). The pH activity profile of Xyl-L was determined in the range of 4–10, showing a maximum of activity in a pH range of 7–9 at 25 °C (Fig. 2B).

The effects on Xyl-L activity of metal ions and other reagents at two different concentrations are shown in Table 1. Only $ZnSO_4$ and EDTA affected significantly the activity of the enzyme, reducing

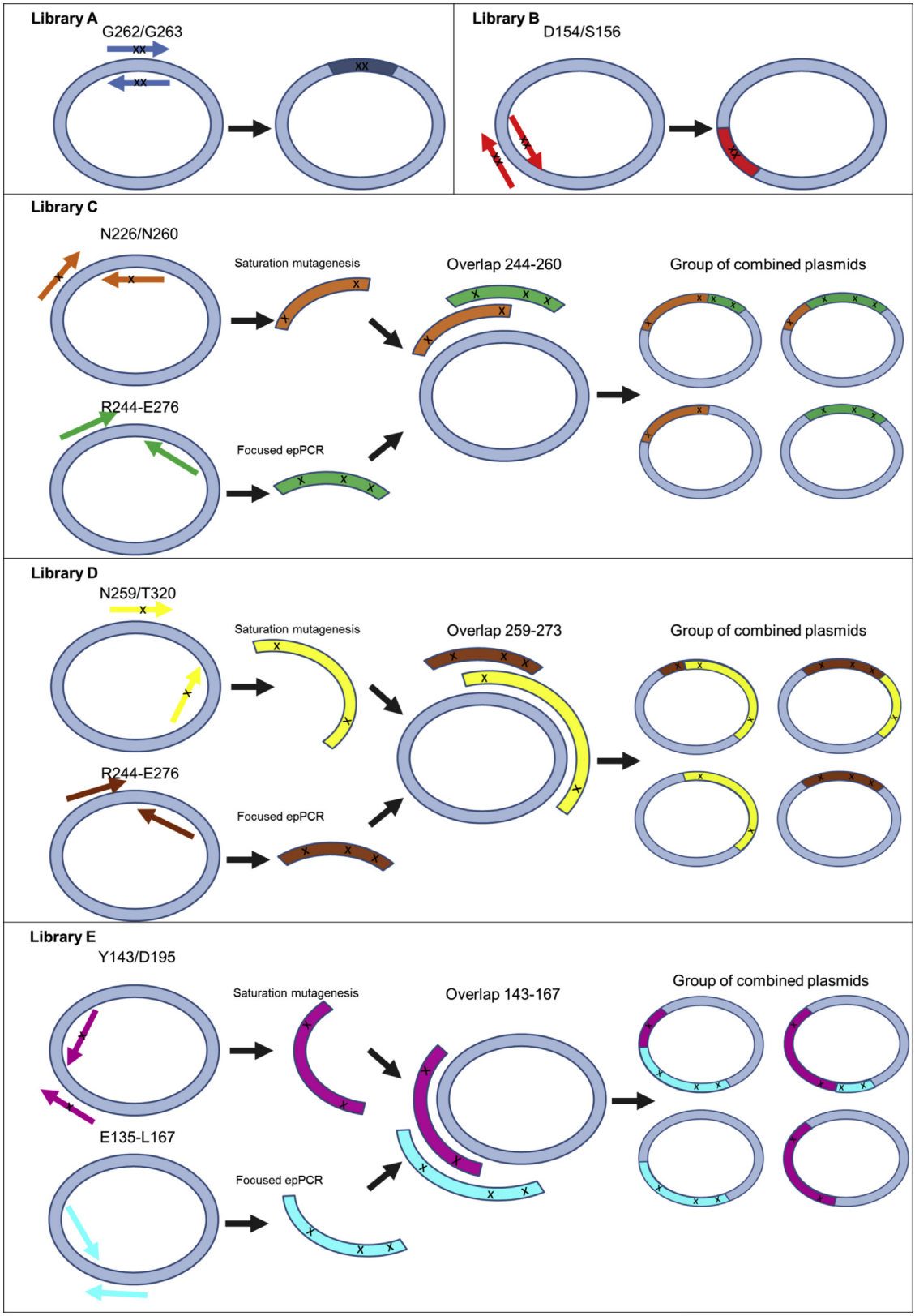

Fig. 1. Schematic representation of the new directed evolution method. As shown in the scheme, plasmid amplification using the two megaprimers in the case of library C, D and E generates four groups of randomized plasmids as a result of amplification using individual or combined megaprimers.

its activity by about 50%. Other reagents had no significant effect, excepting for $CaCl_2$, which showed an enhancement in the activity of the enzyme at 1 mM and 10 mM.

Kinetic parameters of the recombinant xylanase were obtained at different temperature and pH 8, and calculated from a Lineweaver–Burk plot. At 25 °C, Xyl-L gave a K_m value of 4.1 mg/ml, and a k_{cat} of 145.1 s^{-1}, therefore the catalytic efficiency (k_{cat}/K_m)

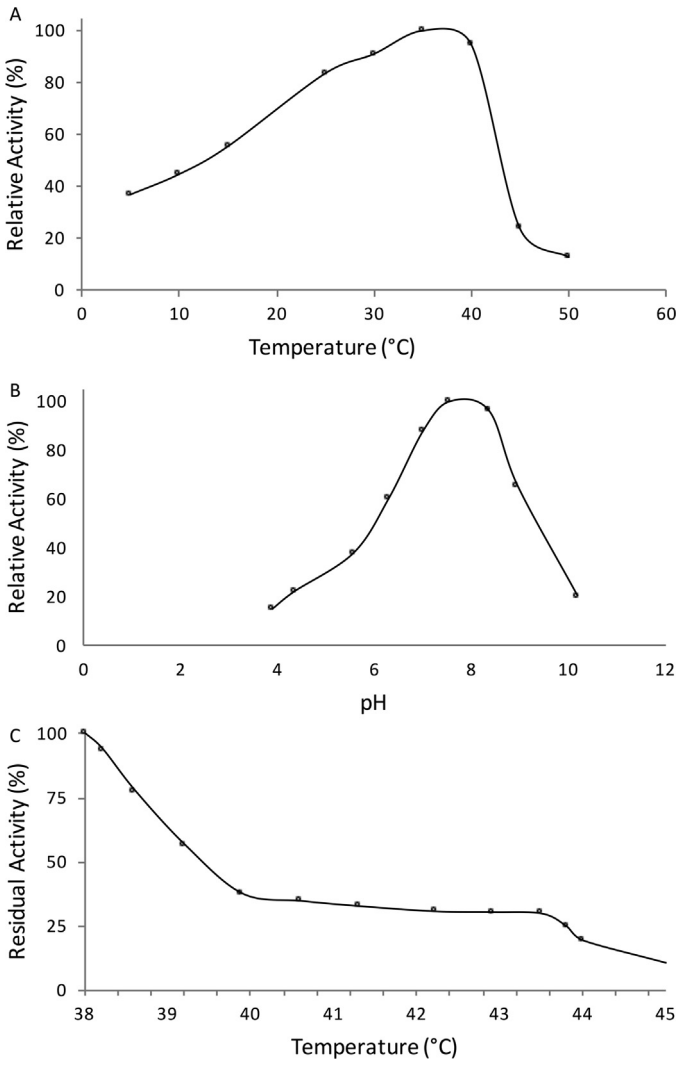

Fig. 2. Effects of temperature and pH on the activity of Xyl-L.
A. Xylanase activity measured at different temperatures using birchwood xylan as substrate at pH 8.0 for 30 min 100% corresponds to maximal hydrolytic activity. B. Xyl-L was incubated with birchwood xylan in 100 mM Britton-Robinson buffer at various pH values at 20 °C for 30 min C. The residual activity of Xyl-L was measured after heat shocks at different temperatures. T5015 was obtained plotting the remaining activity versus the temperature of the heat shock.

Table 1
Effects of different chemicals on Xyl-L activity.

Chemical	Relative activity (%) 1 mM chemical	Relative activity (%) 10 mM chemical
$ZnSO_4$	75	58
$CoCl_2$	101	79
$NiCl_2$	105	77
$CuCl_2$	112	73
$MnCl_2$	108	91
$CaCl_2$	114	120
EDTA	76	52
SDS	106[a]	91[b]
Triton	96[a]	81[b]

[a] 1% of surfactant added.
[b] 10% of surfactant added.

of the Xyl-L for the hydrolysis of birchwood xylan was calculated as 35.4 ml mg^{-1} sec^{-1}. These are promising values, if we compare them with other reported cold-active GH10 xylanases, such as XynA from marine *Glaciecola mesophila* (k_{cat} 61 s^{-1} and K_m 1.42 mg/ml at 30 °C) [57], and r-XynA from *Sorangium cellulosum* (k_{cat} 6 s^{-1} and K_m 27 mg/ml at 30 °C) [58].

The activation energy for the hydrolysis of birchwood xylan in Xyl-L was calculated using the slope of the Arrhenius plot and Arrhenius equation, giving a value of 5.44 kcal/mol in the temperature range from 5 to 35 °C at pH 8.0. This value is lower than the one reported for a xylanase from the psycrophilic yeast *Cryptococcus adeliae* (11.4 kcal/mol) [59]. Activation energies of other enzymes from cold-adapted bacteria have been measured [60] and they have comparable values. The thermostability of Xyl-L was examined by measuring the residual activity at various temperatures (38–45 °C) obtaining a $T_{50}{}^{15}$ value of 39.5 °C, meaning that Xyl-L retained 50% of its activity after 15 min of incubation at 39.5 °C. The stability of the enzyme rapidly decreased at temperatures above 38 °C (Fig. 2C). This thermolabile behavior is a main drawback in the implementation of Xyl-L in a biocatalytic process; therefore, directed evolution based on structural information given by molecular dynamics simulations of a Xyl-L homology model was performed.

3.3. Homology model and molecular dynamics simulations of Xyl-L

Overlap calculation studies had revealed that the structure of GH10 xylanases is more conserved than other GH families [61]. Therefore, a 3D model of the catalytic domain of Xyl-L (343 amino acids) was built on the basis of the resolved structure of three xylanases; Xylanase A from *Streptomyces halstedii* JM8 (1NQ6) [46], with 34% identity; xylanase XYN10A from *Cellvibrio japonicus* (1W32) [47], with 41% identity, and xylanase 10C from *Cellvibrio japonicus* (1US3) [48], with 41% identity. The topology of the modeled structure exhibits a common $(\alpha/\beta)_8$ fold typical of family 10 of glycosyl hydrolases (Fig. 3). The homology model was used for molecular dynamics (MD) simulations of the enzyme. MD simulations gave the root-mean-square deviation (RMSD) values for each residue of the catalytic domain of the enzyme which represents a numerical measure of the differences between all the positions that the residue adopted during the MD simulation. Therefore, residues with a high RMSD value can be selected as flexible amino acids. This strategy is equivalent to the identification of amino acids with higher flexibility using the B-FITTER computer aid, but instead of using the B-factor values extracted from the pdb-file, MD computations were performed, hence the resolved 3D structure is not strictly necessary. This approach uses the deviation of the relative positioning obtained during a MD simulation. In our work, an additional difficulty is the fact that no information other than the nucleotide sequence is provided to perform this type of analysis. This type of strategy has been previously applied to assess conformational flexibility of protein structures [62–64].

3.4. Design and generation of mutagenic libraries

According to the MD simulation results, the most flexible amino acids are located mainly in two regions flanked by residues E135-L167 and R244-E276 (Fig. 4) Each of these regions comprises a loop; M138-V157 and R257-S271, respectively (Fig. 3). Therefore, following the (B-FIT method) and the B-FITTER computer aid [27], an improved thermostability was aimed for by designing and building mutagenic libraries targeting two positions in each flexible region. Using this strategy, we planned to identify hot-spots in a first round of saturation mutagenesis, and then to perform an iterative process of saturation mutagenesis at the selected hot spots [27] or to combine mutations. Following this semi-rational strategy, library A was built using saturation mutagenesis at positions G262 and G263, the two amino acids with the higher RMSD values at the loop R257-S271. Library A was designed based on previous knowledge, that a

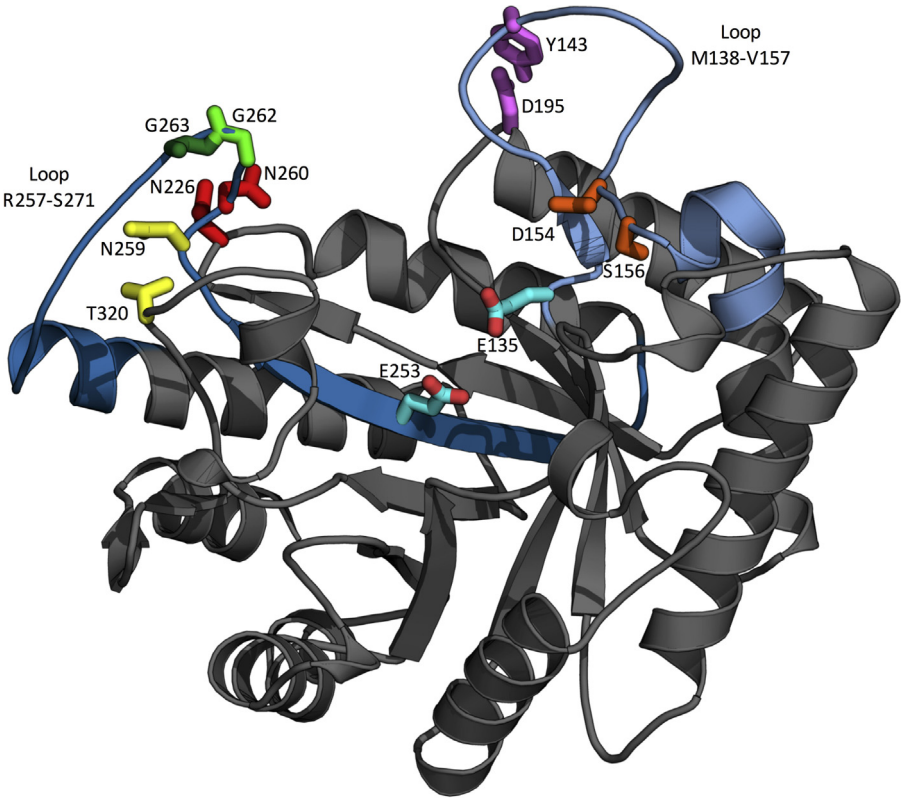

Fig. 3. Ribbon diagram of the catalytic domain of Xyl-L and design of mutagenic libraries.
The topology of the modeled structure exhibits an (α/β)8 fold typical of family 10 of glycosyl hydrolases. The putative catalytic acid-base (E135) and nucleophile (E253) residues are shown. The location of the amino acids for saturation mutagenesis are shown for each library: A (G262 and G263, green), B (D154 and S156, orange), C (N226 and N260, red), D (N259 and T320, yellow) and E (Y143 and D195, violet). Flexible regions identified by MD simulation are highlighted in light blue (E135-L167) and blue (R244-E276). These regions were targeted by focused epPCR for libraries C, D (region R244-E276) and E (region E135-L167).

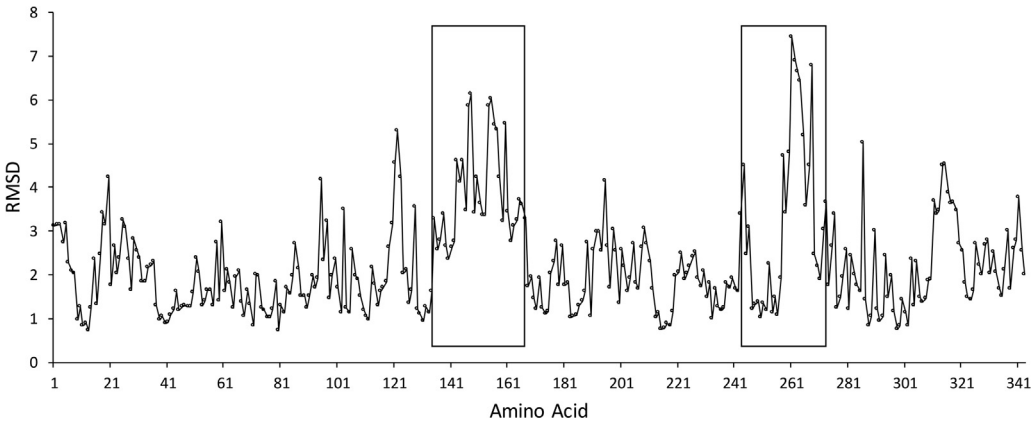

Fig. 4. Identification of flexible regions in Xyl-L for focused epPCR libraries.
The graph shows each amino acid of the catalytic domain with it respective RMSD. Two regions were selected to perform focused epPCR. The regions selected are flanked by residues E135-L167 and R244-E276.

decrease in the number of glycine residues in loops could improve the thermostability of a protein [65]. A second library, library B, was generated to stabilize the loop M138-V157 using the same guidelines. This time, positions D154 and S156 showing the highest RMSD value of the region flanked by residues E135-L167 were randomized using saturation mutagenesis (Fig. 3). For each library, a total of 1536 variants (including four controls per plate) were screened. Activity before and after heat shock at 42 °C for 7 min was measured, and relative and residual activities were calculated for each library variant (Fig. 5). Those mutants showing residual activity higher than 40% under screening conditions (starting parent retained 35% of its activity) and a relative activity above the 50% of the parent activity were selected and tested again by a screening process as described earlier [27]. Among the two libraries, only one variant from library B showed positive results for both criteria. Starting form a fresh culture, the variant was expressed and purified, and activity against Birchwood xylan was measured. $T_{50}{}^{15}$ value for the expressed mutant enzyme was obtained by measuring the residual activity after the heat shock at different temperatures (Table 2). A moderate increase in $T_{50}{}^{15}$ was observed, going from 39.5 °C in the case of the parent mutant to 41.2 °C for the new thermostable variant (See Table 2 and Fig. 6). This mutant was identified

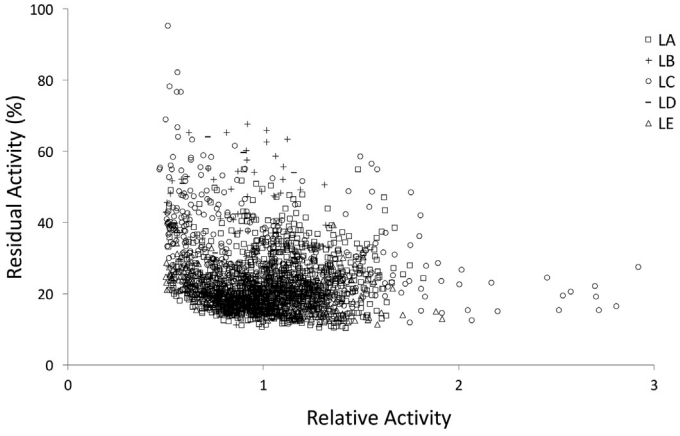

Fig. 5. Relative and residual activity before and after a heat shock of each clone in the five libraries.
Mutant clones with a relative activity higher than 0.5 are plotted against their residual activity after the heat shock. Each library is represented by a different symbol indicated in the legend. Potential hits were screened again under screening reproduction [27].

Table 2
Thermostability of improved xylanase variants found in this work.

Mutant	Mutations[a]	T_{50}^{15}
WT	–	39.5
Lib_B_P4D7	D154P/S156P	41.2
Lib_C_P5F10	V249I	43.8
Lib_C_P8D1	N226L/G262S/I264S	43.6
Lib_C_P7B7	N226H	43.3
Lib_C_P5A2	N260S	42.7
Lib_C_P9H10	N226P	42.0
Lib_D_P1C7	N259L	42.2
Lib_D_P3A5	N259D	41.9
Lib_D_P3C3	N259K/T320N	41.9
Lib_D_P1B8	G262S/T320D	40.5
Lib_D_P1H7	T320M	40.4
Lib_E_P13C6	D195P	40.1

Underlined mutations were introduced by epPCR.
[a] The number of the amino acid mutated correspond to the position in the catalytic domain.

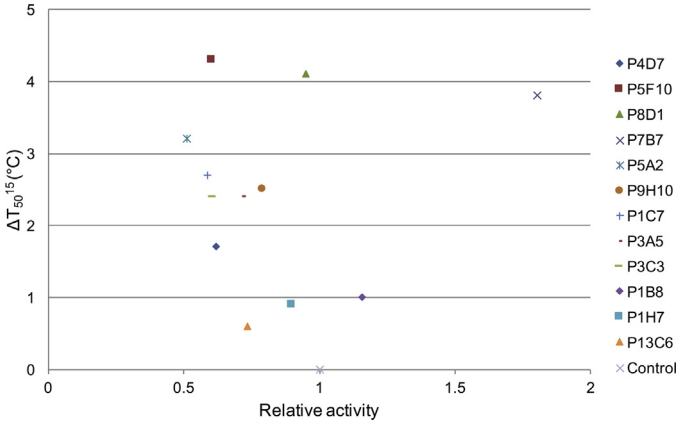

Fig. 6. Relation between the catalityc activity and thermostability of the different selected mutants. Measuring the catalytic activity at 25 °C without previous heat shock treatment, and the thermostability values measured as T_{50}^{15}, a plot was generated to identify the relation between the variants with thermostabilizing mutations and mutations that affect the catalytic activity of the xylanase.

as P4D7 showing interestingly the incorporation of two proline residues (D154P/S156P), which are known as a rigidifying element of loops in protein structures [62]. However, this mutant is not thermostable enough for expanding its application scope. Hence, a different strategy was needed to be applied in order to find several hot spots or several mutants with better thermostability in an iterative step.

A second combined strategy was tested, where saturation libraries are designed to anchor a flexible loop to a rigid part of the protein, as proposed by Vieille & Zeikus (2001) [66]. Accordingly, the randomization of one residue located in a flexible loop and one residue with a low movement rate localized in a structurally rigid region of the protein were considered, while simultaneously randomizing the flexible region comprising the flexible loop in order to amplify the possibilities of creating viable synergistic combinations of mutations.

For the loop R257-S271, two libraries where created using this approach. In library C, the flexible position N260 was randomized together with residue N226 located at a stable region, and in the case of library D, N259 and T320 were subjected to saturated mutations to generate the loop stabilization. In both cases, the positions of the amino acids pairs were chosen according to residue–residue distance feasibility to create molecular interaction between the flexible loop and the rigid part after randomization (Fig. 3). Since randomization positions are located at distant position in the amino acid sequence, two saturation primers were used to create a megaprimer in the library C and D according to the megaprimer method [56]. We wanted to extend the possibility of success in getting thermostability improvement by adding a second megaprimer [56]. This second megaprimer comes from a focused epPCR targeting the flexible regions identified by the RMSD values obtained from the MD simulation (regions flanked by residues E135-L167 and R244-E276 as shown in Fig. 4. In the case of library C and D, focused epPCR was performed between residues R244 and E276 (see Fig. 3, region highlighted in blue). Therefore, two megaprimers containing site saturation mutagenesis and random mutagenesis respectively, will be obtained for this flexible region. Then, the use of these two megaprimers in one megaprimer PCR reaction can be expected to increase the possibility of finding new mutants with improved molecular interactions and thermostability.

Similarly, library E was designed to randomize two residues; Y143 present in the flexible region E135-L167, and D195, the first amino acid of a structurally stable alpha-helix. In this case, focused epPCR was performed between residues E135 and L167 (see Fig. 3, region highlighted in light blue). It is important to ensure the type of randomization obtained when saturation mutagenesis and focused epPCR are used in combination through megaprimer methodology. As explained in Fig. 1, four groups of mutated plasmids are observed during the creation of the libraries; the first one is obtained after plasmid amplification using only the megaprimer created in the saturation mutagenesis step, the second group comes only from the megaprimer created during the focused epPCR, and the third and fourth groups are a combination of both megaprimers generated during the megaprimer PCR reaction. For further clarifying descriptions, see Fig. 1 and material and methods section. Moreover, it is important to notice that positions targeted in library A (G262/G263) and library B (D154/S156), can also be targeted in focused epPCR libraries C/D and E, respectively (Fig. 1).

A total of 1536 transformants per library (including four controls per plate) were screened for libraries C, D and E in the same way as for libraries A and B (Fig. 5). The potential hits of each library were tested again by a screening reproduction [27]. Including the positive hit obtained in library B, twelve mutants showing enhanced thermostability were identify from library B, C, D and E (Fig. 6). The T_{50}^{15} values of each selected mutant enzyme are shown in Table 2. In Fig. 6, T_{50}^{15} values are plotted against the relative catalytic activity of the corresponding variant, highlighting the fact that thermostabilizing mutations can in many cases affect the catalytic activity, as

previously mentioned in several publications [67], and few others can improve the enzymatic performance as well.

4. Discussion

A xylanase encoding gene was isolated from *Psychrobacter* sp. strain 2–17 and cloned into *E. coli* for its heterologous expression. The properties of the recombinant enzyme were found to be consistent with those of a cold-active enzyme; the specific activity was shown to be high at low temperatures. However, the wild-type enzyme was completely inactivated by a moderate increase in temperature. Compared to thermophilic and mesophilic xylanases, the higher efficiency of this enzyme at low to moderate temperature (5–35 °C) was demonstrated, also when compared to other highly active cold-adapted xylanases [57,58,68–70]. An exception is the GH8 cold-active xylanase from *Pseudoalteromonas haloplanktis* [71] that shows similar efficiency as Xyl-L. Although an enzyme with high activity at low temperatures has great potential at the industrial level in application where low temperature reactions are preferred, applications are mostly restricted to food industry. In contrast, important applications in the biofuel and paper industry are limited by the low thermostability of these types of enzyme. Therefore, in this work we used a combination of directed evolution strategies to evolve a highly active enzyme at low to moderate temperature to improve its thermal stability, while keeping or increasing its activity at moderate temperature.

One of the criteria used for directed evolution experiments was based on a B-FIT-like strategy [27], targeting residues with a high degree of flexibility selected by a high RMSD value obtained on the basis of MD simulations of the catalytic domain of Xyl-L. Two saturation mutagenesis libraries were generated, targeting two amino acids in each one with the highest RMSD values (libraries A and B). Among the obtained variants, only one mutant xylanase was identified having a moderate increase in its T_{50}^{15} value, although with reduced catalytic performance. This clearly shows proving the inefficacy of this strategy when used with this particular cold-active enzyme.

In order to increase the possibility of finding positive hits in the screening process, a second strategy was tested. This approach involves random mutagenesis targeting a specific flexible region, (focused epPCR [40]), combined with saturation mutagenesis at two rationally chosen positions. One of the positions comprises a residue with a high RMSD value in a flexible loop, and the other is defined by a nearby residue located in a rigid part of the enzyme (low RMSD value). This strategy was intended to generate mutations in the structural niche where specific saturation mutagenesis occurs in order to increase the chances of creating new stabilizing interaction within the protein structure of the xylanase. Three libraries were generated using this combined strategy. Libraries C and D together provided a total of 10 hits with improved thermostability and variable degree of catalytic performance, and library E one hit.

In library C, five variants were found with T_{50}^{15} between 2.5 and 4.3 °C higher than the parent (Table 2), where three of them resulted from the saturation mutagenesis megaprimer (P7B7 (N226H), P5A2 (N260S), P9H10 (N226P)), one from the focused epPCR megaprimer (P5F10 (V249I)), and finally one from the combination of the two megaprimers (P8D1 (N226L/G262S/I264S)). We analyzed the best variant (P5F10: V249I) in the homology model using Swiss-Prot [49], where a cavity was found to be reduced in its volume in 10 of the 17 possible conformers. This could be an explanation of the enhancement in thermostability, as reported previously by other researches [72,73]. Another hit of this library was thermostabilized to a similar degree (T_{50}^{15} was improved by 4.1 °C) and was found to have three mutations; N226L (consequence of the saturation mutagenesis), and G262S and I264S (produced by the focused epPCR) without showing a variation in the activity at room temperature. It is important to point out that the combination of these three point mutations could not have been generated simply by combining possible hits from separate epPCR and saturation mutagenesis libraries, since neither N226L nor G262S/I264S would have been selected separately during the screening step of each library for later combination. In simultaneous combination during the one-step megaprimer PCR reaction, they were selected possibly due to synergistic effects.

For library D, five hit variants with T_{50}^{15} between 0.9 and 2.7 °C higher than the parent were found (Table 2), where four of them resulted from the saturation mutagenesis megaprimer (P1C7 (N259L), P3A5 (N259D), P3C3 (N259 K/T320N), P1H7 (T320 M)) and one from the combination of the two megaprimers (P1B8 (G262S/T320D)). In the case of library E, the performance of the combined strategy was less efficient, getting only one hit from the saturation mutagenesis megaprimer (P13C6 (D195P)).

In library C, mutants with amino acids modifications at location 226 in the sequence showed either increased or reduced catalytic activity, meaning this spot could be relevant not only for thermostabilization but catalytic performance as well. In the case of library D, amongst the mutants having modifications at the "thermostability" locations 259 or 260, catalytic activity was adversely affected notably, showing that this position is not a good location for mutations.

Importantly, our results show that it is possible to improve the thermostability of the Xyl-L without losing activity at 25 °C, and in some mutants (e.g. P7B7) getting a significant improvement in catalysis as well (Fig. 6).

In this study, the cold-active xylanase proved to be a challenging enzyme to thermostabilize using at least the B-FIT strategy with a limited screening effort, unlike other examples of enzymes in the literature [27,74]. In contrast, the combination of saturation mutagenesis and focused epPCR at individual steps of mutant generation proved to be successful, while still using a minimal number of clones during the screening. This particular one-step strategy allows the identification of combinations of mutantations from mutual epPCR/saturation randomization that otherwise would not be selected by sequential rounds of mutagenesis/screening of both methods separately. To the best of our knowledge, this strategy has not been explored previously. It is a viable alternative to other recently developed thermostabilization strategies [75]. We expect that the combined approach will find applications in future studies of other enzymes with focus on thermostability, but also on stereoselectivity [16,25,76].

Acknowledgements

This work was supported by the Millennium Scientific Initiative, Project ICM PO5-001-F and the basal Centre CeBiB of Conicyt (FB0001). We would also like to thank the support of the Max-Planck-Institut für Kohlenforschung where the protein engineering part of this work was completed, as well as Prof. César A. Ramírez-Sarmiento for helpful discussions and helping with the artwork

Appendix A. Supplementary data

Supplementary data associated with this article can be found, in the online version, at http://dx.doi.org/10.1016/j.enzmictec.2017.02.005.

References

[1] S. D'Amico, P. Claverie, T. Collins, D. Georlette, E. Gratia, A. Hoyoux, et al., Molecular basis of cold adaptation.: Philos, Trans. R. Soc. Lond. B: Biol. Sci. 357 (2002) 917–925.
[2] G. Feller, C. Gerday, Psychrophilic enzymes: hot topics in cold adaptation, Nat. Rev. Microbiol. 1 (2003) 200–208.
[3] G. Feller, Protein stability and enzyme activity at extreme biological temperatures, J. Phys. Condens. Matter. 22 (2010) 323101.
[4] N.J. Russell, Toward a molecular understanding of cold activity of enzymes from psychrophiles, Extremophiles 4 (2000) 83–90.
[5] D. Georlette, V. Blaise, F. Bouillenne, B. Damien, S.H. Thorbjarnardóttir, E. Depiereux, et al., Adenylation-dependent conformation and unfolding pathways of the NAD+-dependent DNA ligase from the thermophile *Thermus scotoductus*, Biophys. J. 86 (2004) 1089–1104.
[6] C. Gerday, M. Aittaleb, M. Bentahir, J.P. Chessa, P. Claverie, T. Collins, et al., Cold-adapted enzymes: from fundamentals to biotechnology, Trends Biotechnol. 18 (2000) 103–107.
[7] N.J. Russell, Molecular adaptations in psychrophilic bacteria: potential for biotechnological applications, Adv. Biochem. Eng. Biotechnol. 61 (1998) 1–21.
[8] R. Margesin, G. Feller, Biotechnological applications of psychrophiles., Environ. Technol., 31 (n.d.) 835–44.
[9] M. Santiago, C.A. Ramírez-Sarmiento, R.A. Zamora, L.P. Parra, Discovery molecular mechanisms and industrial applications of cold-Active enzymes, Front. Microbiol. 7 (2016) 1408.
[10] M.F. Cole, E.A. Gaucher, Utilizing natural diversity to evolve protein function: applications towards thermostability, Curr. Opin. Chem. Biol. 15 (2011) 399–406.
[11] V.G.H. Eijsink, S. Gåseidnes, T.V. Borchert, B. van den Burg, Directed evolution of enzyme stability, Biomol. Eng. 22 (2005) 21–30.
[12] A.S. Bommarius, A. Karau, Deactivation of formate dehydrogenase (FDH) in solution and at gas-liquid interfaces., Biotechnol. Prog. 21, (n.d.) 1663–72.
[13] F.H. Arnold, Combinatorial and computational challenges for biocatalyst design, Nature 409 (2001) 253–257.
[14] M.T. Reetz, The importance of additive and non-additive mutational effects in protein engineering, Angew. Chem. Int. Ed. Engl. 52 (2013) 2658–2666.
[15] W.L. Tang, H. Zhao, Industrial biotechnology: tools and applications, Biotechnol. J. 4 (2009) 1725–1739.
[16] U.T. Bornscheuer, G.W. Huisman, R.J. Kazlauskas, S. Lutz, J.C. Moore, K. Robins, Engineering the third wave of biocatalysis, Nature 485 (2012) 185–194.
[17] M.T. Reetz, J.D. Carballeira, A. Vogel, Iterative saturation mutagenesis on the basis of B factors as a strategy for increasing protein thermostability, Angew. Chem. Int. Ed. Engl. 45 (2006) 7745–7751.
[18] O. Kuchner, F.H. Arnold, Directed evolution of enzyme catalysts, Trends Biotechnol. 15 (1997) 523–530.
[19] G.C. Rice, D.V. Goeddel, G. Cachianes, J. Woronicz, E.Y. Chen, S.R. Williams, et al., Random PCR mutagenesis screening of secreted proteins by direct expression in mammalian cells, Proc. Natl. Acad. Sci. U. S. A. 89 (1992) 5467–5471.
[20] W.P. Stemmer, DNA shuffling by random fragmentation and reassembly: in vitro recombination for molecular evolution, Proc. Natl. Acad. Sci. U. S. A. 91 (1994) 10747–10751.
[21] K. Miyazaki, F.H. Arnold, Exploring nonnatural evolutionary pathways by saturation mutagenesis: rapid improvement of protein function, J. Mol. Evol. 49 (1999) 716–720.
[22] D.A. Estell, T.P. Graycar, J.A. Wells, Engineering an enzyme by site-directed mutagenesis to be resistant to chemical oxidation, J. Biol. Chem. 260 (1985) 6518–6521.
[23] A.S. Bommarius, Biocatalysis: a status report, Annu. Rev. Chem. Biomol. Eng. 6 (2015) 319–345.
[24] K.A. Powell, S.W. Ramer, S.B. Del Cardayré, W.P.C. Stemmer, M.B. Tobin, P.F. Longchamp, et al., Directed evolution and biocatalysis, Angew. Chem. Int. Ed. Engl. 40 (2001) 3948–3959.
[25] M.T. Reetz, Laboratory evolution of stereoselective enzymes: a prolific source of catalysts for asymmetric reactions, Angew. Chem. Int. Ed. Engl. 50 (2011) 138–174, http://dx.doi.org/10.1002/anie.201000826.
[26] M.T. Reetz, M. Bocola, J.D. Carballeira, D. Zha, A. Vogel, Expanding the range of substrate acceptance of enzymes: combinatorial active-site saturation test, Angew. Chem. Int. Ed. Engl. 44 (2005) 4192–4196.
[27] M.T. Reetz, J.D. Carballeira, Iterative saturation mutagenesis (ISM) for rapid directed evolution of functional enzymes, Nat. Protoc. 2 (2007) 891–903.
[28] J.D. Bloom, S.T. Labthavikul, C.R. Otey, F.H. Arnold, Protein stability promotes evolvability, Proc. Natl. Acad. Sci. U. S. A. 103 (2006) 5869–5874.
[29] R. Ruller, L. Deliberto, T.L. Ferreira, R.J. Ward, Thermostable variants of the recombinant xylanase A from *Bacillus subtilis* produced by directed evolution show reduced heat capacity changes, Proteins 70 (2008) 1280–1293.
[30] J. Ni, M. Takehara, M. Miyazawa, H. Watanabe, Random exchanges of non-conserved amino acid residues among four parental termite cellulases by family shuffling improved thermostability, Protein Eng. Des. Sel. 20 (2007) 535–542.
[31] T. Collins, C. Gerday, G. Feller, Xylanases, xylanase families and extremophilic xylanases, FEMS Microbiol. Rev. 29 (2005) 3–23.
[32] S. Subramaniyan, P. Prema, Biotechnology of microbial xylanases: enzymology, molecular biology, and application, Crit. Rev. Biotechnol. 22 (2002) 33–64.
[33] Bajpai, Application of enzymes in the pulp and paper industry, Biotechnol. Prog. 15 (1999) 147–157.
[34] K. Miyazaki, M. Takenouchi, H. Kondo, N. Noro, M. Suzuki, S. Tsuda, Thermal stabilization of Bacillus subtilis family-11 xylanase by directed evolution, J. Biol. Chem. 281 (2006) 10236–10242.
[35] Z.-G. Zhang, Z.-L. Yi, X.-Q. Pei, Z.-L. Wu, Improving the thermostability of *Geobacillus stearothermophilus* xylanase XT6 by directed evolution and site-directed mutagenesis, Bioresour. Technol. 101 (2010) 9272–9278.
[36] P. Biely, M. Vrsanská, M. Tenkanen, D. Kluepfel, Endo-beta-1,4-xylanase families: differences in catalytic properties, J. Biotechnol. 57 (1997) 151–166.
[37] H. van Tilbeurgh, G. Pettersson, R. Bhikabhai, H. De Boeck, M. Claeyssens, Studies of the cellulolytic system of *Trichoderma reesei* QM 9414. Reaction specificity and thermodynamics of interactions of small substrates and ligands with the 1,4-beta-glucan cellobiohydrolase II, Eur. J. Biochem. 148 (1985) 329–334.
[38] L.P. Parra, F. Reyes, J.P. Acevedo, O. Salazar, B.A. Andrews, J.A. Asenjo, Cloning and fusion expression of a cold-active lipase from marine Antarctic origin, Enzyme Microb. Technol. 42 (2008) 371–377.
[39] J.P. Acevedo, F. Reyes, L.P. Parra, O. Salazar, B.A. Andrews, J.A. Asenjo, Cloning of complete genes for novel hydrolytic enzymes from Antarctic sea water bacteria by use of an improved genome walking technique, J. Biotechnol. 133 (2008) 277–286.
[40] A. Gratz, J. Jose, Protein domain library generation by overlap extension (PDLGO): A tool for enzyme engineering, Anal. Biochem. 378 (2008) 171–176.
[41] R.M. Teather, P.J. Wood, Use of Congo red-polysaccharide interactions in enumeration and characterization of cellulolytic bacteria from the bovine rumen, Appl. Environ. Microbiol. 43 (1982) 777–780.
[42] M.M. Bradford, A rapid and sensitive method for the quantitation of microgram quantities of protein utilizing the principle of protein-dye binding, Anal. Biochem. 72 (1976) 248–254.
[43] C. Breuil, J.N. Saddler, Comparison of the 3,5-dinitrosalicylic acid and Nelson-Somogyi methods of assaying for reducing sugars and determining cellulase activity, Enzyme Microb, Technol 7 (1985) 327–332.
[44] H.T.S. Britton, R.A. Robinson, CXCVIII.—universal buffer solutions and the dissociation constant of veronal, J. Chem. Soc. 0 (1931) 1456–1462.
[45] A. Sali, T.L. Blundell, Comparative protein modelling by satisfaction of spatial restraints, J. Mol. Biol. 234 (1993) 779–815.
[46] A. Canals, M.C. Vega, F.X. Gomis-Rüth, M. Díaz, R. óN. I. Santamaría, M. Coll, Structure of xylanase Xys1delta from *Streptomyces halstedii*, Acta Crystallogr. D: Biol. Crystallogr. 59 (2003) 1447–1453.
[47] S.R. Andrews, E.J. Taylor, G. Pell, F. Vincent, V.M.-A. Ducros, G.J. Davies, et al., The use of forced protein evolution to investigate and improve stability of family 10 xylanases. The production of Ca2+-independent stable xylanases, J. Biol. Chem. 279 (2004) 54369–54379.
[48] G. Pell, L. Szabo, S.J. Charnock, H. Xie, T.M. Gloster, G.J. Davies, et al., Structural and biochemical analysis of *Cellvibrio japonicus* xylanase 10C: how variation in substrate-binding cleft influences the catalytic profile of family GH-10 xylanases, J. Biol. Chem. 279 (2004) 11777–11788.
[49] N. Guex, M.C. Peitsch, SWISS-MODEL and the Swiss-PdbViewer: an environment for comparative protein modeling, Electrophoresis 18 (1997) 2714–2723.
[50] L.O.B. J.A. Asenjo, B.A. Andrews, J.P. Acevedo, L.P. Parra, Protein and DNA sequence encoding a cold adapted xylanase, US8679814 B2, (2014).
[51] S. Wu, J.P. Acevedo, M.T. Reetz, Induced allostery in the directed evolution of an enantioselective Baeyer-Villiger monooxygenase, Proc. Natl. Acad. Sci. U. S. A. 107 (2010) 2775–2780.
[52] K. Bowers, E. Chow, H. Xu, R. Dror, M. Eastwood, B. Gregersen, et al., Scalable Algorithms for Molecular Dynamics Simulations on Commodity Clusters, In: ACM/IEEE SC 2006 Conf., IEEE, (2006) pp. 43–43.
[53] J. Hsin, A. Arkhipov, Y. Yin, J.E. Stone, K. Schulten, Using VMD: an introductory tutorial, Curr. Protoc. Bioinf. (2008) (Chapter 5, Unit 5.7).
[54] S. Kille, C.G. Acevedo-Rocha, L.P. Parra, Z.-G. Zhang, D.J. Opperman, M.T. Reetz, et al., Reducing codon redundancy and screening effort of combinatorial protein libraries created by saturation mutagenesis, ACS Synth. Biol. 2 (2013) 83–92.
[55] H.H. Hogrefe, J. Cline, G.L. Youngblood, R.M. Allen, Creating randomized amino acid libraries with the QuikChange multi site-directed mutagenesis kit, Biotechniques 33 (2002) 1158–1160 (1162, 1164-5).
[56] J. Sanchis, L. Fernández, J.D. Carballeira, J. Drone, Y. Gumulya, H. Höbenreich, et al., Improved PCR method for the creation of saturation mutagenesis libraries in directed evolution: application to difficult-to-amplify templates, Appl. Microbiol. Biotechnol. 81 (2008) 387–397.
[57] B. Guo, X.-L. Chen, C.-Y. Sun, B.-C. Zhou, Y.-Z. Zhang, Gene cloning expression and characterization of a new cold-active and salt-tolerant endo-beta-1,4-xylanase from marine Glaciecola mesophila KMM 241, Appl. Microbiol. Biotechnol. 84 (2009) 1107–1115.
[58] S.-Y. Wang, W. Hu, X.-Y. Lin, Z.-H. Wu, Y.-Z. Li, A novel cold-active xylanase from the cellulolytic myxobacterium *Sorangium cellulosum* So9733-1: gene cloning, expression, and enzymatic characterization, Appl. Microbiol. Biotechnol. 93 (2012) 1503–1512.
[59] I. Petrescu, J. Lamotte-Brasseur, J.P. Chessa, P. Ntarima, M. Claeyssens, B. Devreese, et al., Xylanase from the psychrophilic yeast *Cryptococcus adeliae*, Extremophiles 4 (2000) 137–144.
[60] Y. Morita, T. Nakamura, Q. Hasan, Y. Murakami, K. Yokoyama, E. Tamiya, Cold-active enzymes from cold-adapted bacteria, J. Am. Oil Chem. Soc. 74 (1997) 441–444.

[61] V. Ducros, S.J. Charnock, U. Derewenda, Z.S. Derewenda, Z. Dauter, C. Dupont, et al., Substrate specificity in glycoside hydrolase family 10. Structural and kinetic analysis of the Streptomyces lividans xylanase 10A, J. Biol. Chem. 275 (2000) 23020–23026.
[62] H. Yu, Y. Zhao, C. Guo, Y. Gan, H. Huang, The role of proline substitutions within flexible regions on thermostability of luciferase, Biochim. Biophys. Acta 1854 (2015) 65–72.
[63] Y. Xie, J. An, G. Yang, G. Wu, Y. Zhang, L. Cui, et al., Enhanced enzyme kinetic stability by increasing rigidity within the active site, J. Biol. Chem. 289 (2014) 7994–8006.
[64] J. Wang, Z. Tan, M. Wu, J. Li, J. Wu, Improving the thermostability of a mesophilic family 10 xylanase AuXyn10A, from *Aspergillus usamii* by in silico design, J. Ind. Microbiol. Biotechnol. 41 (2014) 1217–1225.
[65] G. Vogt, S. Woell, P. Argos, Protein thermal stability hydrogen bonds, and ion pairs, J. Mol. Biol. 269 (1997) 631–643.
[66] C. Vieille, G.J. Zeikus, Hyperthermophilic enzymes: sources, uses, and molecular mechanisms for thermostability, Microbiol. Mol. Biol. Rev. 65 (2001) 1–43.
[67] P.A. Romero, F.H. Arnold, Exploring protein fitness landscapes by directed evolution, Nat. Rev. Mol. Cell Biol. 10 (2009) 866–876.
[68] S. Chen, M.G. Kaufman, K.L. Miazgowicz, M. Bagdasarian, E.D. Walker, Molecular characterization of a cold-active recombinant xylanase from *Flavobacterium johnsoniae* and its applicability in xylan hydrolysis, Bioresour. Technol. 128 (2013) 145–155.
[69] X. Liu, Z. Huang, X. Zhang, Z. Shao, Z. Liu, Cloning, expression and characterization of a novel cold-active and halophilic xylanase from *Zunongwangia profunda*, Extremophiles 18 (2014) 441–450.
[70] J. Zhou, Y. Liu, J. Shen, R. Zhang, X. Tang, J. Li, et al., Kinetic and thermodynamic characterization of a novel low-temperature-active xylanase from *Arthrobacter sp*. GN16 isolated from the feces of Grus nigricollis, Bioengineered 6 (2015) 111–114.
[71] T. Collins, M.-A. Meuwis, I. Stals, M. Claeyssens, G. Feller, C. Gerday, A novel family 8 xylanase, functional and physicochemical characterization, J. Biol. Chem. 277 (2002) 35133–35139.
[72] E. Baldwin, J. Xu, O. Hajiseyedjavadi, W.A. Baase, B.W. Matthews, Thermodynamic and structural compensation in size-switch core repacking variants of bacteriophage T4 lysozyme, J. Mol. Biol. 259 (1996) 542–559.
[73] S. Knapp, W.M. de Vos, D. Rice, R. Ladenstein, Crystal structure of glutamate dehydrogenase from the hyperthermophilic eubacterium *Thermotoga maritima* at 3.0 A resolution, J. Mol. Biol. 267 (1997) 916–932.
[74] J.K. Blum, M.D. Ricketts, A.S. Bommarius, Improved thermostability of AEH by combining B-FIT analysis and structure-guided consensus method, J.Biotechnol 160 (2012) 214–221.
[75] H.J. Wijma, R.J. Floor, P.A. Jekel, D. Baker, S.J. Marrink, D.B. Janssen, Computationally designed libraries for rapid enzyme stabilization, Protein Eng. Des. Sel. 27 (2014) 49–58.
[76] M.T. Reetz, Directed Evolution of Selective Enzymes, Wiley-VCH Verlag GmbH & Co KGaA, Weinheim, Germany, 2016.